PrP(C) association with lipid rafts in the early secretory pathway stabilizes its cellular conformation.

Daniela Sarnataro, Vincenza Campana, Simona Paladino, Mariano Stornaiuolo, Lucio Nitsch, Chiara Zurzolo

Molecular Biology of the Cell
Vol. 15, 4031–4042, September 2004

PrP^C Association with Lipid Rafts in the Early Secretory Pathway Stabilizes Its Cellular Conformation[D]

Daniela Sarnataro,*† Vincenza Campana,*†‡ Simona Paladino,*‡ Mariano Stornaiuolo,§ Lucio Nitsch,* and Chiara Zurzolo*‡‖

*Dipartimento di Biologia e Patologia Cellulare e Molecolare, Centro di Endocrinologia ed Oncologia Sperimentale del Consiglio Nazionale delle Ricerche, Università degli Studi di Napoli Federico II, 80131 Napoli, Italy; ‡Unité de Trafic Membranaire et Pathogénèse, Institut Pasteur, 75724 Paris Cedex 15, France; §Dipartimento di Biochimica e Biotecnologie Mediche, Università degli Studi di Napoli Federico II, 80131 Napoli, Italy

Submitted May 2, 2003; Revised June 4, 2004; Accepted June 22, 2004
Monitoring Editor: Keith Mostov

The pathological conversion of cellular prion protein (PrP^C) into the scrapie prion protein (PrP^{Sc}) isoform appears to have a central role in the pathogenesis of transmissible spongiform encephalopathies. However, the identity of the intracellular compartment where this conversion occurs is unknown. Several lines of evidence indicate that detergent-resistant membrane domains (DRMs or rafts) could be involved in this process. We have characterized the association of PrP^C to rafts during its biosynthesis. We found that PrP^C associates with rafts already as an immature precursor in the endoplasmic reticulum. Interestingly, compared with the mature protein, the immature diglycosylated form has a different susceptibility to cholesterol depletion vs. sphingolipid depletion, suggesting that the two forms associate with different lipid domains. We also found that cholesterol depletion, which affects raft-association of the immature protein, slows down protein maturation and leads to protein misfolding. On the contrary, sphingolipid depletion does not have any effect on the kinetics of protein maturation or on the conformation of the protein. These data indicate that the early association of PrP^C with cholesterol-enriched rafts facilitates its correct folding and reinforce the hypothesis that cholesterol and sphingolipids have different roles in PrP metabolism.

INTRODUCTION

Transmissible spongiform encephalopathies (TSEs) are neurodegenerative diseases characterized by the accumulation in the brain of the misfolded form of cellular prion protein (PrP^C), a cellular glycosylphosphatidylinositol (GPI)-anchored protein highly conserved among many species (Piccardo *et al.*, 1998; Chabry *et al.*, 1999; Wopfner *et al.*, 1999). It has been proposed that a direct interaction between the correctly folded PrP^C form and the infectious misfolded protein (scrapie prion protein [PrP^{Sc}]) is required for the conformational transition to occur (Kocisko *et al.*, 1994; Harris, 1999; Horiuchi and Caughey, 1999).

This transconformation could occur either at the plasma membrane (Caughey *et al.*, 1989, 1991; Kaneko *et al.*, 1997), where the protein is normally localized, or in the endolysosomal compartment (Caughey and Raymond, 1991; Borchelt *et al.*, 1992; Taraboulos *et al.*, 1995; Jeffrey *et al.*, 2000; Magalhaes *et al.*, 2002). Indeed, after being exported to the plasma membrane (Borchelt *et al.*, 1990; Harris, 1999) PrP^C is internalized (Shyng *et al.*, 1994; Vey *et al.*, 1996) and can recycle back to the surface (Taraboulos *et al.*, 1992; Harris, 1999; Prado *et al.*, 2004). Furthermore, in some cases misfolded PrP^{Sc} protein has been found to accumulate in lysosomes (Laszlo *et al.*, 1992; Jeffrey *et al.*, 2000), suggesting an involvement of the endolysosomal compartment in the transconformational event (Borchelt *et al.*, 1992). However, it has also been shown that the misfolded prion protein is subject to proteasomal degradation, being retrotranslocated from the ER (Ma and Lindquist, 2001). Furthermore PrP cytosolic variants are present in amorphous aggregates and assume a PrP^{Sc}-like conformation, which are highly neurotoxic in transgenic mice (Ma *et al.*, 2002; Ma and Lindquist, 2002).

Although the precise compartment where conformational transition occurs has not yet been identified, it has been proposed that lipid rafts are involved (Taraboulos *et al.*, 1995; Vey *et al.*, 1996; Naslavsky *et al.*, 1997, 1999; Prusiner *et al.*, 1998; Harris, 1999). Lipid rafts are dynamic lipid assemblies enriched in cholesterol and sphingolipids. They are

Article published online ahead of print. Mol. Biol. Cell 10.1091/mbc.E03–05–0271. Article and publication date are available at www.molbiolcell.org/cgi/doi/10.1091/mbc.E03–05–0271.

[D] Online version of this article contains supporting material. Online version is available at www.molbiolcell.org.

† These authors contributed equally to this work.

‖ Corresponding author. E-mail addresses: zurzolo@unina.it; zurzolo@pasteur.fr.

Abbreviations used: BiP, binding protein; βCD, methyl-β-cyclodextrin; CLT, calreticulin; CNX, calnexin; DRMs, detergent-resistant membrane domains; Endo-H, endoglycosidase-H; ER, endoplasmic reticulum; FB1, fumonisin B1; FRT, Fischer rat thyroid; GPI, glycosylphosphatidylinositol; Mev, mevinolin; PK, proteinase K; PDI, protein disulfide isomerase; PrP^C, cellular prion protein; PrP^{Sc}, scrapie prion protein; TGN, *trans*-Golgi network; TNE, Tris/NaCl/EDTA; TSEs, transmissible spongiform encephalopathies; TX-100, Triton X-100.

able to segregate laterally forming phase domains that are more liquid-ordered (Simons and Ikonen, 1997; Brown and London, 1998; van der Goot and Harder, 2001) compared with adjacent membranes, which are enriched in more unsaturated and short-chained phospholipids (Simons and Ikonen, 1997; Brown and London, 1998; Kuzchalia and Parton, 1999). Like other GPI-anchored proteins (Brown and Rose, 1992; Tiveron *et al.*, 1994; Zurzolo *et al.*, 1994; Lipardi *et al.*, 2000), both PrP^{C} and PrP^{Sc} have been found enriched in rafts and are typically resistant to extraction in cold Triton X-100 (TX-100; Taraboulos *et al.*, 1992; Naslavsky *et al.*, 1997; Harris, 1999) and are able to float in the lighter fractions on sucrose density gradients (Naslavsky *et al.*, 1997; Sarnataro *et al.*, 2002). Furthermore, Taraboulos *et al.* (1995) have shown that cellular cholesterol depletion, which impairs association of PrP^{C} with rafts, inhibits the formation of the scrapie form in infected ScN2a neuroblastoma cells. Conversely, the same group has shown that sphingolipid depletion facilitates the conversion process (Naslavsky *et al.*, 1999). Moreover, infectious prion rods were found to contain the sphingolipids Galactosylceramide (Gal/Cer) and Sphingomyelin (SM), which are characteristic lipid components of rafts (Klein *et al.*, 1998; Mahfoud *et al.*, 2002). All together these data suggest that raft-enriched lipids may interact with the normal and/or the pathogenic prion protein and that rafts might be the site of scrapie formation.

We have previously transfected PrP^{C} from mouse (moPrP^{C}) in polarized epithelial Fischer rat thyroid (FRT) cells and studied its exocytic trafficking (Sarnataro *et al.*, 2002). We have demonstrated that in these cells PrP^{C} associates with DRMs. However, cholesterol depletion does not affect its transport to the plasma membrane (Sarnataro *et al.*, 2002), thus excluding a role for rafts in the exocytic transport, as is typical for other GPI-anchored proteins (Brown *et al.*, 1989; Lisanti *et al.*, 1989; Brown and Rose, 1992; Brown and London, 1998; Lipardi *et al.*, 2000).

We have further analyzed the properties of PrP^{C} raft-association in order to define its functional significance. We found that PrP^{C} associates with DRMs early during its biosynthesis and that its different biosynthetic forms are differently affected by cholesterol and sphingolipid depletion. We also found that impairment of raft-association by cholesterol depletion during the early stage of PrP biosynthesis leads to protein misfolding in the ER. On the contrary, when raft-association of the mature form is impaired by sphingolipid depletion, folding of the protein is not affected. These data strongly suggest a functional role for the early raft-association of PrP in assisting its correct folding in the endoplasmic reticulum and possibly point to a specific role of cholesterol in this process.

MATERIALS AND METHODS

Reagents and Antibodies

Cell culture reagents were purchased from Life Technologies Laboratories (Grand Island, NY). The PRI 308 antibody and SAF 32 antibody were a kind gift of Dr. J. Grassi (CEA, Service depharmacologie et d'immunologie, Gif-sur-Yvette, France). Protein A-Sepharose was from Pharmacia Diagnostics AB (Uppsala, Sweden). The antibodies against binding protein (BiP), calnexin (CNX), calreticulin (CLT), protein disulfide isomerase (PDI), and endosomal marker EEA1 were from StressGen Biotechnologies Corp. (Victoria, British Columbia, Canada). The antibodies against ribophorin I (RibI) and giantin were kind gifts from Dr. Stefano Bonatti (Dipartimento di Biologia e Biotecnologie Mediche, Università degli Studi di Napoli "Federico II," Italy). The antibody against GM130 was from Santa Cruz Biotechnology (Santa Cruz, CA). The antibody against caveolin 1 was from BD Transduction Laboratories (Lexington, KY). Methyl-β-cyclodextrin (βCD), mevinolin, and all other reagents were obtained from Sigma Chemical Co. (St. Louis, MO).

PrP Construct and Transfection

FRT cells were transfected with a cDNA encoding 3F4 tagged moPrP^{C}, a kind gift of Dr. Sylvain Lehmann (Institut deGenetique Humaine, UPR CNRS1142, Montpellier, France), with the calcium phosphate procedure, as previously described (Zurzolo *et al.*, 1993). Stable clones were selected by G418 resistance.

Cell Culture and Drug Treatment

FRT cells stably expressing moPrP^{C} were grown in F12 Coon's modified medium containing 5% FBS. Mevinolin and βCD treatments were carried out as described elsewhere (Keller and Simons, 1998). Briefly, FRT cells were plated on dishes and mevinolin (10 μM for 48 h) was added to the cells 24 h after plating in F12 supplemented with 5% delipidated calf serum and mevalonate (200 μM). FRT cells were allowed to grow for another 48 h. βCD (10 mM) was added to the medium containing 20 mM HEPES, pH 7.5, and 0.2% bovine albumin for 1 h at 37°C to cells pretreated with mevinolin/mevalonate for 48 h. For sphingolipid depletion FRT cells were grown in the presence of fumonisin B1 (FB1, 25 μg/ml) for 72 h. FB1 was added in fresh F12 medium 4 h after plating cells and changed after 48 h of culture.

Cholesterol Determination

To assay cholesterol levels in the cells before and after treatment with mevinolin/mevalonate and βCD, we used two different methods.

1) FRT cells grown in the presence or absence of mevinolin/mevalonate, as described above, were washed twice with PBS and cholesterol-labeling medium (3.3 μCi [H^3]cholesterol in F12 in the absence or presence of mevinolin/mevalonate) was added for 8 h at 37°C. Cells were then washed in PBS and incubated in cholesterol-labeling medium with or without mevinolin/mevalonate for an additional 20 h. The cells were then treated for 60 min at 37°C with 10 mM βCD. [H^3]cholesterol remaining in the cells was determined by liquid scintillation counting (model LS60000SC; Beckman Instruments, Fullerton, CA).

2) Alternatively, we used a colorimetric assay. FRT cells grown in the presence or absence of mevinolin/mevalonate were washed twice with PBS, lysed with appropriate lysis buffer and Infinity Cholesterol Reagent (Sigma Chemical Co.; code number 401-25 P) was added to the lysates in the ratio 1:10 for 5 min at 37°C (according to the suggested Sigma protocol number 401). The samples were then measured in a spectrophotometer at 550 nm.

Assays for DRM Association

Sucrose Density Gradients. Sucrose gradient analysis of TX-100–insoluble material was performed using previously published protocols (Brown and Rose, 1992). Cells were grown to confluence in 100-mm dishes, washed in PBS C/M, and lysed for 20 min in TNE/TX-100 1% buffer (25 mM Tris-HCl [pH 7.5], 150 mM NaCl, 5 mM EDTA, 1% TX-100) on ice. Lysates were scraped from dishes, brought to 40% sucrose and then placed at the bottom of a centrifuge tube. A sucrose gradient (5–35% TNE) was layered on top of the lysates, and the samples were centrifuged at 39,000 rpm for 18–20 h in an ultracentrifuge (model SW41; Beckman Instruments). One-milliliter fractions were harvested from the top of the gradient. PrP^{C} was revealed by Western blotting using the SAF 32 antibody.

Sucrose Density Gradient after Pulse-chase and Immunoprecipitation. Cells plated in 100-mm dishes (3 for each chase time) were pulsed for 20 min with 100 μCi/ml [^{35}S]methionine and chased for various times at 37°C, as indicated in Figures 2 and 4. At the end of the chase times the cells were washed with cold PBS and lysed for 20 min in TNE/TX-100 1% buffer on ice, brought to 40% sucrose, and then placed at the bottom of the tube. Flotation on sucrose gradient (5–35% TNE) was then performed as described before. The fractions recovered from the top of the gradient were immunoprecipitated for 16 h by SAF 32 antibody coupled to protein A-Sepharose beads. The pellets were washed twice with cold lysis buffer and three times with PBS. The samples were then boiled with SDS-sample buffer, loaded on 12% polyacrylamide gels, and revealed by phosphorimager scanning.

Sucrose Density Gradient on Purified ER Fraction. ER microsomes (~1–1.5 mg; prepared as indicated below) were resuspended and lysed for 20 min in 2 ml of TXE/TX-100 1% buffer on ice and floated on sucrose density gradient, as above. The fractions were TCA precipitated or immunoprecipitated by using SAF 32 antibody and loaded on 12% polyacrylamide gels. Western blots were performed using anti-EEA1, -GM130, -CNX, -PDI, -BiP and -RibI antibodies. For the labeled samples, the immunoprecipitated PrP was revealed by scanning at phosphorimager.

Endoglycosidase-H Digestion

Digestion with endoglycosidase-H (Endo-H) was carried out on immunoprecipitated materials for 16 h at 37°C (Endo-H 5 mU/sample). The immunoprecipitates were first boiled for 3 min in 50 μl of 0.1 M sodium citrate, pH 5.5, containing 0.1% SDS and then treated with Endo-H (Thotakura and Bahl, 1987). The samples were then resuspended in SDS-sample buffer, boiled, and loaded on 12% polyacrylamide gels and revealed by fluorography.

GM1 Determination

A drop of 30 μl of each sucrose gradient fraction was spotted on nitrocellulose membrane, applying vacuum for few seconds. The membrane was saturated for 2 h in 5% milk in PBS/0.1% Tween and then incubated 1 h with cholera toxin-HRP (Sigma) and revealed by ECL.

ER Microsome Purification

ER microsome purification was performed modifying a previously published protocol (Ying *et al.*, 2000). FRT cells were grown into dishes of 150-mm diameter and harvested at 80–90% confluence and eventually labeled for 20 min with 100 μCi/ml [^{35}S]methionine. Then they were washed twice with ice-cold PBS and pelleted by centrifugation for 10 min at 800 rpm in an Allegra 6KR centrifuge (Beckman Coulter) at 4°C. The pellet was resuspended in to 800 μl of Buffer F (0.25 M sorbitol, 10 mM HEPES-KOH, pH 7.2, 10 mM KAc, 1.5 mM MgAc) and homogenized by 10 passages through a 22-gauge needle. The nuclei and cell debris were sedimented by centrifugation for 5 min at 600 × *g* in an Eppendorf centrifuge. The postnuclear supernatant was quantified and 50, 100, or 300 μg of protein was used to test the concentration of different markers by immunoblotting (total homogenate, see Figure 3). About 4–7 mg of total proteins were adjusted to 0.75 M sorbitol and centrifuged 12 min at 16,000 rpm at 4°C in a Ti75i rotor in a Beckman ultracentrifuge. ER microsomes were lysed 20 min in TXE/TX-100 1% buffer on ice and proteins were quantified. Fifty, 100, or 300 μg of protein was used to blot for different intracellular markers in comparison with total homogenate (see Figure 3).

Immunoprecipitation of Molecular Chaperones

Cells grown in 60-mm dishes were washed three times with PBS and lysed in JS buffer (1% TX-100, 150 mM NaCl, 1% Glycerol, 50 mM HEPES, pH 7.5, 1.5 mM $MgCl_2$, 5 mM EGTA), protease inhibitor cocktail (leupeptin, antipain, pepstatin, and 1 mM PMSF) for 20 min, scraped from dishes, and put into microfuge tubes. The lysates were then precleared with protein A-Sepharose beads (5 mg/sample) for 30 min and incubated overnight at 4°C with BiP, CNX, CLT, or PDI. The pellets were washed twice with cold lysis buffer and three times with PBS. The samples were then boiled with SDS-sample buffer, loaded on appropriate polyacrylamide gels and revealed by Western blotting against PrP and ECL.

Assays for Scrapie-like Properties

Triton/Doc Insolubility Assay. Cells were lysed in Triton/Doc buffer (0.5% TX-100, 0.5% Na-deoxycholate, 150 mM NaCl, and 100 mM Tris, pH 7.5) for 20 min and cleared lysates were centrifuged at 265,000 × *g* for 40 min in a TLA 100.3 rotor using a Beckman Optima TL ultracentrifuge. PrP^C was recovered in the supernatants and pelleted by TCA precipitation. It has been shown that in these conditions only PrP^{Sc} but not PrP^C from brain extracts and cell culture lysates (from CHO, NIH 3T3, or neuroblastoma cells) sediments (Lehmann and Harris, 1996a, 1996b; Lehmann and Harris, 1997; Priola and Chesebro, 1998).

Proteinase K Digestion Assay. To measure proteinase K (PK)-resistance, lysates (without a protease inhibitor cocktail) were digested with (3.3 μg/ml) for different times at 37°C, as indicated. The proteins were TCA precipitated and then analyzed for PrP by immunoblotting with PRI 308 antibody. The conditions used for proteinase digestion are identical to those previously published (Lehmann and Harris, 1996a, 1996b; Lehmann and Harris, 1997; Priola and Chesebro, 1998).

Fluorescence Microscopy

FRT cells stably expressing PrP^C were grown for 4–5 days on coverslips, washed with PBS, fixed in 2% paraformaldehyde, permeabilized with 0.075% saponin, and processed for indirect immunofluorescence using specific antibody. PrP^C was visualized by using TRITC-conjugated secondary antibodies, whereas giantin and CLT were revealed by using FITC-conjugated secondary antibodies using a Zeiss Laser Scanning Confocal Microscope (LSCM 410 or 510; Thornwood, NY).

Cell Fractionation

FRT cells (plated in 12 150-mm dishes) were homogenized by 10 strokes in an isobiotec cell homogenizer with a tungsten-carbide ball (clearance of 12 μm) in 500 μl of 20 mM HEPES/KOH, pH 7.3, and 120 mM sucrose. A postnuclear supernatant fraction was obtained by centrifugation at 600 × *g* for 5 min in an Eppendorf centrifuge. The postnuclear supernatant was loaded on top of a discontinuous sucrose gradient (0.6 ml each of 15, 20, 25, 30, 35, 40, and 45% with 0.5 ml of 60% on the bottom) made up in the same buffer. The gradient was spun in an SW 50.1 rotor for 1 h at 45,000 rpm in a Beckman ultracentrifuge and 14 fractions were collected from the bottom of the tube with a peristaltic pump. The same fractions of the different gradients were pulled and 1/20 of each was loaded on 12% polyacrylamide gels. Western blots were performed using first anti-PrP antibody and then anti-RibI and anti-GM130 antibodies.

PK resistance was tested for fractions 1, 2, and 3 (representative of ER) and 5, 6, and 7 (of Golgi apparatus) in control and cholesterol depletion conditions.

RESULTS

Effect of Cholesterol and Sphingolipid Depletion on PrP^C Association with DRMs

We have recently shown that $moPrP^C$ transfected in FRT cells associates with lipid rafts and that this association is cholesterol dependent (Sarnataro *et al.*, 2002). Indeed, we demonstrated that cholesterol depletion affects the characteristic insolubility of PrP^C in cold extraction buffer containing 1% TX-100. However, we also demonstrated that cholesterol depletion does not affect the delivery of PrP^C to the basolateral domain of the plasma membrane of FRT cells (where it normally resides), thus excluding a canonical role for DRMs in TGN sorting and exocytic transport of the protein.

To better characterize raft-association of PrP^C in FRT cells and to define the functional role of this association, we purified PrP^C on sucrose density gradients in control cells and in conditions previously shown to perturb raft-association of proteins (Keller and Simons, 1998; Lipardi *et al.*, 2000; Sarnataro *et al.*, 2002; Figure 1A). We therefore depleted the cells either of cholesterol, using a combined treatment of mevinolin and βCD (Mev/βCD) or of sphingolipids, using fumonisin B1 (FB1; Taraboulos *et al.*, 1995; Keller and Simons, 1998; Naslavsky *et al.*, 1999; Sarnataro *et al.*, 2002). We found that both cholesterol (Figure 1A, Mev/βCD) and sphingolipid depletion (Figure 1A, FB1) affected the rate of PrP^C flotation to the lighter fractions of sucrose gradients (Figure 1A). However, the effect was quite distinct for the different isoforms of the protein. Although the mature form (H) was equally affected by cholesterol and sphingolipid depletion (going from ~58% flotation in control conditions to ~34% and ~35% in cholesterol and sphingolipid depletion, respectively; Figure 1B), the immature diglycosylated isoform (I*), which has been described as the major ER precursor of the mature protein (Caughey *et al.*, 1989; Petersen *et al.*, 1996; Capellari *et al.*, 1999; Sarnataro *et al.*, 2002), had a very different behavior in the two conditions. Although its flotation was increased from ~30 to ~60% in cholesterol-depleted cells, it was reduced to undetectable levels by FB1 treatment (Figure 1A). Quantitation of the effects of cholesterol and sphingolipid depletion on the two forms are shown in Figure 1B, which represents the results of four independent experiments. These data could indicate that the mature and immature forms of PrP^C associate with different lipid domains that are characterized by distinct susceptibilities to cholesterol and sphingolipid depletion.

It is interesting to note that a typical raft marker, caveolin 1, in FRT cells cotransfected with *cav1* and PrP^C genes behaves similarly to the PrP^C mature isoform and reduces its flotation in both cholesterol and sphingolipid depletion (Supplemental Figure 1).

PrP^C Associates with DRMs Early in its Secretory Pathway

Because we and others (Caughey *et al.*, 1989; Petersen *et al.*, 1996; Capellari *et al.*, 1999) have shown that the immature diglycosylated form of PrP^C (I*) is the major precursor of the mature form (H) and is found mainly in the ER (Sarnataro *et al.*, 2002), we sought to better characterize the association of PrP^C with DRMs during its biosynthesis. To assess the tim-

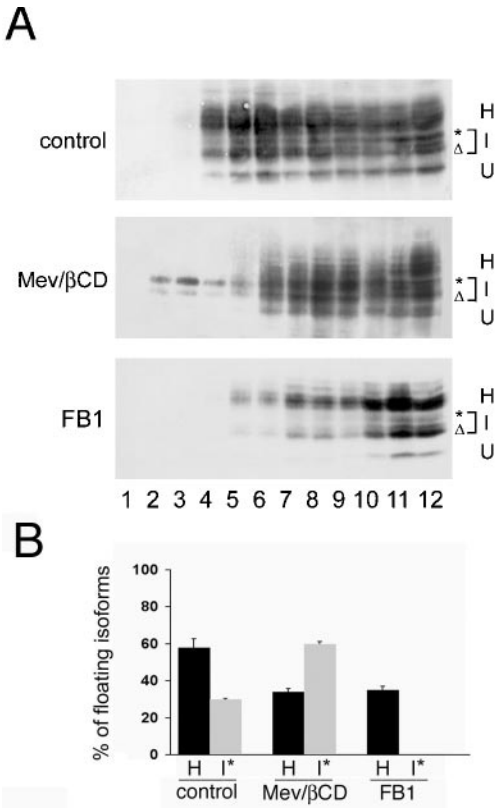

Figure 1. Effect of cholesterol and sphingolipid depletion on PrP^C association with DRMs. (A) FRT cells were grown to confluence on 100-mm dishes and treated or not (control) with mevinolin and β-cyclodextrin (Mev/βCD) or fumonisin B1 (FB1) as previously described (Taraboulos *et al.,* 1995; Keller and Simons, 1998; Naslavsky *et al.,* 1999). The cells were lysed for 20 min in cold TNE/TX-100 buffer and then run through a discontinuous 5–40% sucrose gradient. One-milliliter fractions (12 fractions in total) were collected from the top to bottom of the tube after centrifugation to equilibrium, and PrP^C was TCA precipitated from all fractions, loaded on 12% gels, and revealed by Western blotting with a specific antibody and ECL. (B) The data from four independent experiments were quantified using NIH image for Macintosh and plotted as shown in the graphs. The amount of PrP present in each fraction of the gradients is considered as percentage of the total amount of the protein in all fractions. In the graph is reported only the floating amount of H and I* PrP isoforms (fractions 1–7 of the gradients). Error bars are indicated. H, mature, highly glycosylated PrP^C isoform; I*, unmodified diglycosylated isoform; I^{Δ}, monoglycosylated form; U, unglycosylated form (Capellari *et al.,* 1999; Sarnataro *et al.,* 2002).

ing of this association, we performed sucrose density gradient purification after TX-100 extraction during pulse-chase experiments (Figure 2). We found that the immature diglycosylated (I*) precursor floated to the lighter fractions of the gradients already after a 20-min pulse, at chase time 0. By quantifying three different experiments we calculated that at 0 chase ~30% of the I* form was floating (Figure 2, right panel, time 0). Because at this time the protein was completely sensitive to Endo-H treatment (Figure 2, middle panel), these data show that the immature I* form associates with DRMs before the medial Golgi (i.e., between the ER and the early Golgi). After 15 min of chase the band corresponding to the immature diglycosylated form (I*) began to disappear as the mature form (H) appeared, confirming that this was the major ER precursor of the mature protein. Interestingly at this time, when the protein began to become Endo-H resistant (indicating its passage into the medial Golgi), the mature protein (H) began to associate with the floating fractions (~ 30%, as indicated in the right panel). At this chase time the monoglycosylated form (I^{Δ}) and the unglycosylated U form also associated with DRMs, and this association continued to increase with time for all three H, I^{Δ}, and U forms. These data are consistent with previous findings showing that these three isoforms are exported to the plasma membrane in FRT as well as in N2a cells (Borchelt *et al.,* 1990; Harris, 1999; Sarnataro *et al.,* 2002). On the contrary the immature diglycosylated form (I*) completely disappeared after 30 min of chase, therefore confirming that it does not reach the surface and is fully converted into the mature form (Caughey *et al.,* 1989; Petersen *et al.,* 1996; Capellari *et al.,* 1999).

As a control for DRM association we used GM1, an extensively characterized raft marker (Parton, 1994; Mayor and Maxfield, 1995). The flotation profile of GM1 was obtained by spotting an aliquot of each fraction on nitrocellulose membranes followed by hybridization with cholera toxin-HRP (Figure 2, bottom panel).

Because Endo-H resistance does not permit to discriminate between ER and early Golgi, in order to assess whether DRM association of PrP in the early secretory pathway occurred already in the ER, we performed a flotation assay for PrP after purification of ER membranes (Figure 3; Dhanvantari and Loh, 2000). ER microsomes were prepared from FRT cells by cellular fractionation (as described in *Materials and Methods*) and were characterized by blotting with antibodies against specific markers of different intracellular organelles to evaluate enrichment in the ER membrane and the grade of contamination by other intracellular membranes. The same amount of total cell homogenate and of the microsomal preparation (normalized for protein concentration) was used in the blotting and compared (Figure 3A). We found that although in the microsomal fraction very little (between 0 and 5% of total homogenate) of the endosomal marker EEA1 (Bartlett *et al.,* 2001; Kauppi *et al.,* 2002) was found, GM130 (*cis*-Golgi marker; Nakamura *et al.,* 1995; Taguchi *et al.,* 2003) was totally absent (Figure 3A). On the contrary, four different ER-specific markers, CNX (Jackson *et al.,* 1994), PDI (Narindrasorasak *et al.,* 2003), BiP (Paulsson and Wang, 2003), and RibI (Nigam, 1990) were present in an amount corresponding respectively to 65, 54, 55, and 50% of the total homogenate, therefore demonstrating a good grade of purity of ER membranes in the purified microsomal fractions. In agreement with these results, an amount corresponding to 40% of the total homogenate was found for the immature PrP I* isoform in a similar preparation of the microsomal fraction pulse labeled for 20 min and immunoprecipitated with specific anti-PrP antibody (Figure 3A).

To assess whether the PrP I* isoform present in the ER microsomes associated with DRMs, we labeled the cells for 20 min before microsomal purification, because the maximal amount of this transitory form is found in these conditions, as shown in the pulse chase experiment of Figure 2. The microsomal membranes were then resuspended and lysed in cold TNE-TX-100 1% buffer and immediately immunoprecipitated with anti-PrP antibody (Figure 3A) or subjected to flotation on sucrose density gradients (Figure 3B).

We found that ~20% of the PrP I* isoform floated in the lighter fractions of the gradients (Figure 3B). The discrepancy between the floating amounts of the I* isoform in purified ER (20%) and in pulse-chase and flotation derived from total cells (30%, see Figure 2) is probably due

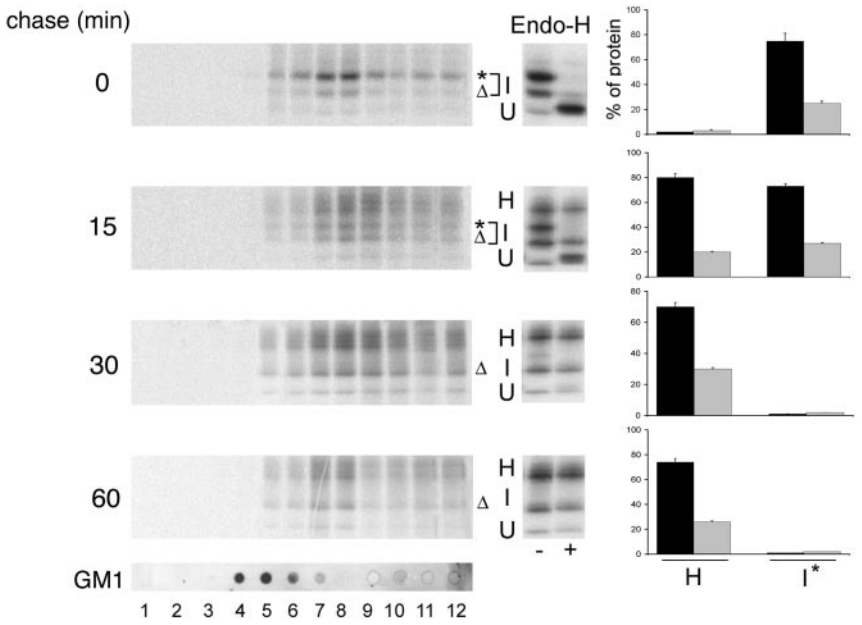

Figure 2. Association of PrP^C with DRMs in the early secretory pathway. FRT cells grown on 100-mm dishes (3 dishes for each chase time) were pulsed for 20 min with [^{35}S]methionine and then chased for the indicated times. The cells were lysed in TNE/TX-100 1% buffer and then run through a linear 5–40% sucrose gradient. One-milliliter fractions were collected from the top to bottom of the tube after centrifugation to equilibrium, and PrP^C was immunoprecipitated from all fractions with SAF 32 antibody and subjected to SDS-PAGE and phosphorimager scanning (left panel). The amount of PrP^C in each fraction was quantified by scanning three independent gels using the NIH image software for Macintosh and is represented in right panel as percentage of the total amount of the protein (gray bars indicate the amount of floating PrP^C, fractions 1–7; black bars indicate the amount of soluble PrP^C, fractions 8–12). Endo-H treatment (Thotakura and Bahl, 1987), performed after every chase time on an aliquot of the sample before running the sucrose gradient, is shown in the middle panel. Error bars are indicated. H, mature, highly glycosylated PrP^C isoform; I*, unmodified diglycosylated isoform; I^{Δ}, monoglycosylated form; U, unglycosylated form. Raft fractions are identified by the GM1 profile on sucrose density gradient, shown at the bottom of the picture.

to a loss of membranes during the ER purification procedure and possibly to a different sensitivity of the purified ER membranes to TX-100 extraction. Differently from the immature PrP, RibI was unable to float on the gradient derived from the microsomal membrane (Figure 3B). Flotation profiles in the total cellular lysate of the markers for the different intracellular compartments are also shown (Figure 3C).

These experiments clearly demonstrate that a purified ER fraction contains the I* PrP precursor in DRMs. This characteristic was specific for this immature form because we were not able to find other floating proteins among all the ER markers tested (RibI, Figure 3B; PDI, BiP, and CNX, unpublished data).

Effect of Cholesterol and Sphingolipid Depletion on PrP^C Maturation

The fact that a major precursor (I*) of the protein not subsequently found at the plasma membrane associated with DRMs early during its biosynthesis was of major interest and hinted to a possible role of raft-association in PrP^C maturation. To test this hypothesis, we followed PrP^C biosynthesis by pulse-chase experiments in conditions of cholesterol and sphingolipid depletion (Figure 4A). We found that in cholesterol-depleted cells the I* precursor form was present at up to 30 min chase and remained Endo-H sensitive. In contrast FB1 treatment did not have any effect, because the I* immature precursor rapidly disappeared after

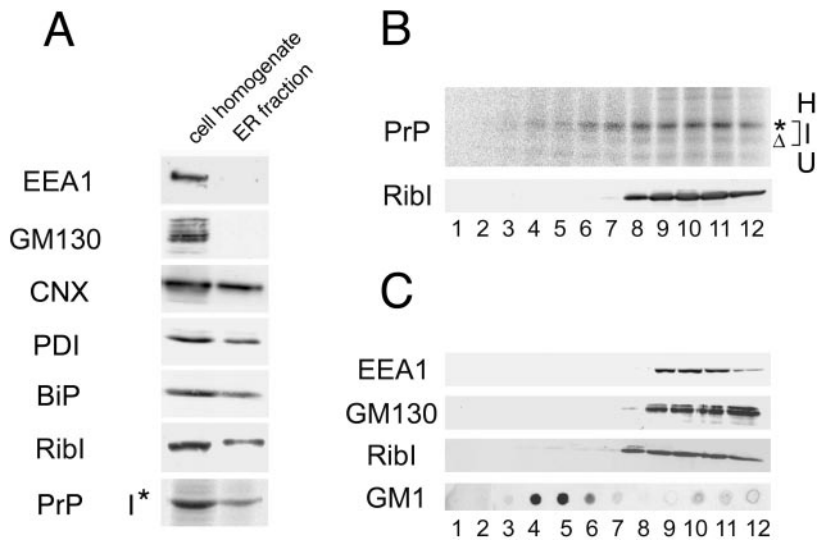

Figure 3. Analysis of PrP^C in DRMs from purified ER membranes. (A) ER microsomes were purified from FRT cells grown on 150-mm dishes as described in *Materials and Methods*. Fifty or 100 μg of proteins in the cell homogenate and in the microsomal fraction were TCA precipitated, subjected to SDS-PAGE, and blotted using anti-EEA1, -GM130, -CNX, -PDI, -BiP, and -RibI antibodies. PrP^C was revealed after immunoprecipitation with SAF 32 antibody by phosphorimager scanning from 300 μg of ER microsomes isolated as above after a 20-min pulse with [^{35}S]methionine. (B) ER microsomes obtained after pulse-labeling the cells for 20 min with [^{35}S]methionine were lysed in cold TNE/TX-100 1% buffer and the run through a discontinuous 5–40% sucrose density gradient. The collected fractions were immunoprecipitated with SAF 32, loaded on 12% gel, and revealed by phophorimager scanning. The flotation profile of RibI by western blot of TCA-precipitated fractions of a sucrose density gradient of ER microsomes is shown below. (C) Flotation profile of different intracellular markers, e.g., EEA1, GM130, RibI, and GM1 from the total cellular lysate in TNE/TX-100 1% is shown for comparison.

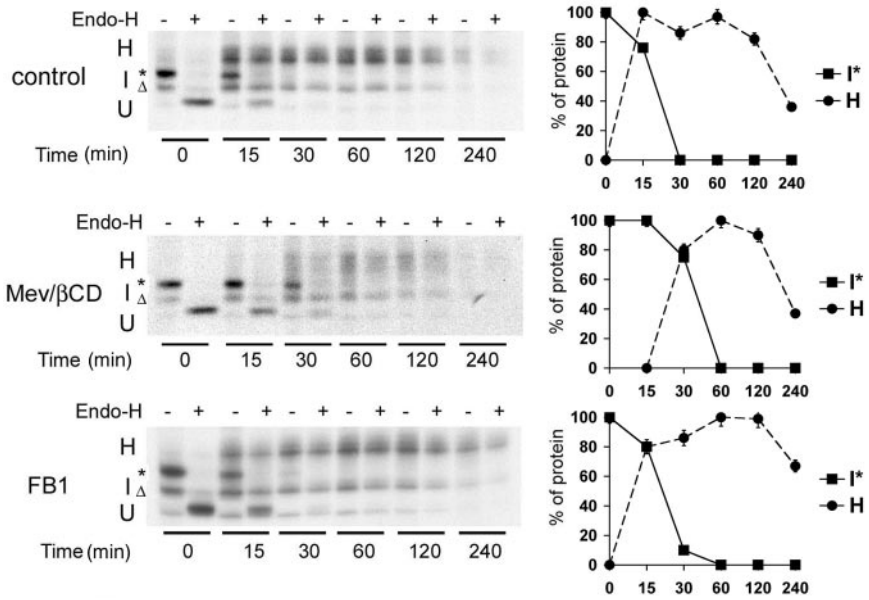

Figure 4. Pulse-chase analysis of PrP^C after cholesterol and sphingolipid depletion. FRT cells grown in control (control), cholesterol depletion (Mev/βCD), and sphingolipid depletion (FB1) conditions (see *Materials and Methods*) were subjected to pulse-chase analysis by using [^{35}S]methionine for the indicated times. At the end of each chase time the cells were lysed in Triton/Doc buffer and PrP^C was immunoprecipitated with SAF 32 antibody. The immunoprecipitated material was treated (+) or not (−) with Endo-H (5 mU/sample for 16 h at 37°C). The protein was revealed by SDS-PAGE and phosphorimager scanning. Quantitation of four independent experiments are shown in the graphs in the right panels. Error bars are reported from the different quantitations. H, mature, highly glycosylated PrP^C isoform; I*, unmodified diglycosylated isoform; I^{Δ}, monoglycosylated form; U, unglycosylated form.

15 min of chase with kinetics similar to that in control cells (Figure 4). Furthermore, compared with control cells the appearance of the mature form (H) was delayed only in cholesterol- but not in sphingolipid-depleted cells (Figure 4, graphs in the right panel). These results have been consistently reproduced several times, and we were able to quantify the effect of cholesterol depletion on the kinetics of PrP maturation as a delay of ~30 min. Because these effects were specific for cholesterol and not for sphingolipid depletion, these data indicated that perturbation of DRM association of the I* precursor, as a result of cholesterol depletion, could affect the maturation process of the protein.

Role of DRM Association in PrP^C Folding

To understand whether association of the precursor form of PrP with DRMs in the ER was involved in determining the correct folding of the protein, we sought to check whether in conditions of perturbation of rafts the protein remained associated with the ER chaperones. We tested whether PrP^C coimmunoprecipitated with either BiP, PDI, CNX, and CLT in control and cholesterol- or sphingolipid-depleted FRT cells (Figure 5). We found that although in control cells and in cells treated with FB1 the amount of PrP^C that coimmunoprecipitated with the ER chaperones was negligible, PrP^C coimmunoprecipitated with all the ER chaperones tested after cholesterol depletion. By quantification of three different experiments we calculated that in cholesterol-depleted cells ~5–10% of the total protein coimmunoprecipitated with the different chaperones. Thus, in conditions of cholesterol depletion a portion of the protein was interacting with the ER chaperones, which might be indicative of incorrect folding.

To then directly test whether PrP^C was correctly folded, we subjected the cells to PK treatment and to extraction in Triton/Doc and analyzed the behavior of PrP^C in these two conditions. These two assays are also used to identify the scrapie-like characteristics of PrP and its mutants because they reveal an abnormal folding of the protein (Lehmann and Harris, 1996a, 1996b, 1997; Priola and Chesebro, 1998).

We found that only in conditions of cholesterol depletion did the protein become partially misfolded (Figure 6A). Indeed, by quantification of several independent experiments we calculated that ~30% of PrP^C became resistant to 2 min of PK treatment and a similar amount was recovered in the pellet after ultracentrifugation of Triton/Doc lysates in cholesterol-depleted cells (Figure 6B). These data are consistent with the data shown in Figure 5 and indicate that in

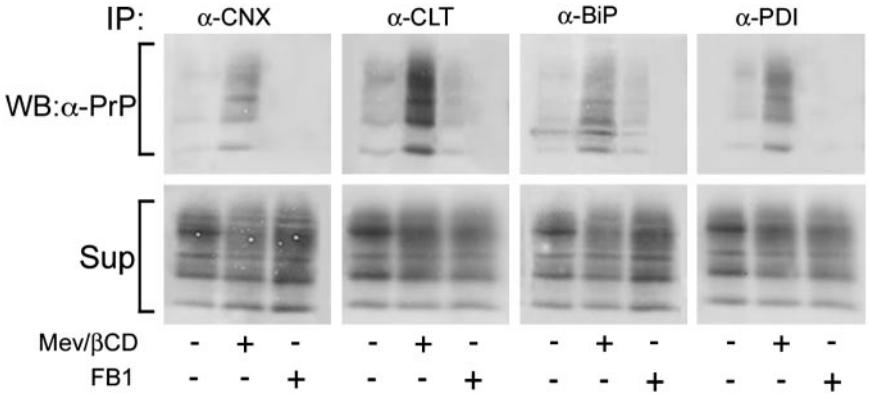

Figure 5. Analysis of PrP^C interaction with ER chaperones. FRT cells were plated in 35-mm dishes in control (−), cholesterol depletion (Mev/βCD +), or sphingolipid depletion (FB1 +) conditions. The cells were then lysed in JS buffer and BiP, PDI, CNX, and CLT were immunoprecipitated (IP) in nondenaturing conditions with the specific antibodies (see *Materials and Methods*). The immunoprecipitates and 1/10 of the supernatants (Sup) were loaded on polyacrylamide gels. The gels were revealed for the presence of PrP^C by Western blotting with the specific antibody (WB:α-PrP) by ECL.

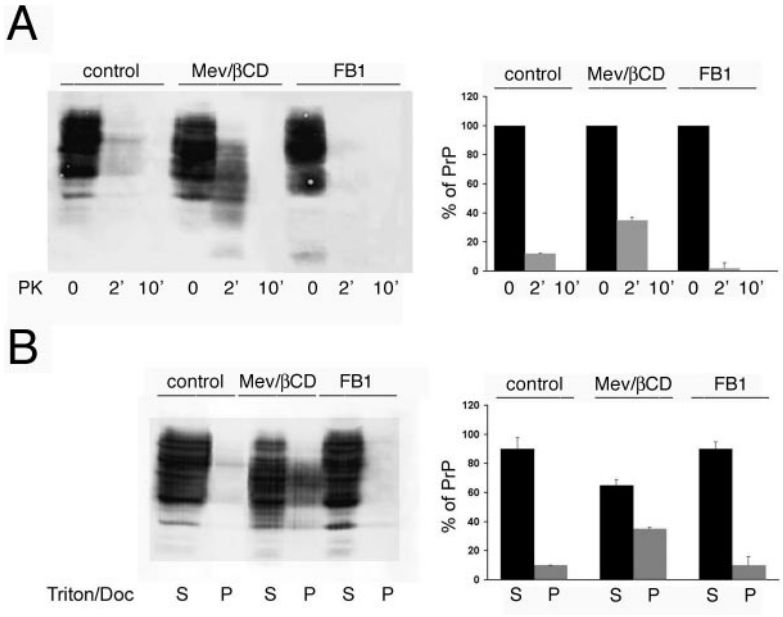

Figure 6. Analysis of PrP^C misfolding in FRT cells. FRT cells were grown in 35-mm dishes in control (control), cholesterol (Mev/βCD), or sphingolipid (FB1) depletion conditions. The cells were lysed in Triton/Doc buffer, in the absence of proteases inhibitors, and where indicated were treated with PK (3.3 μg/ml) for 2 or 10 min (A) or centrifuged in a TLA 100.3 rotor at 265,000 × *g* and separated into soluble (S) and insoluble (P) materials (B). In both cases PrP^C was revealed by Western blotting by using specific antibodies and ECL. The data were also quantified using the NIH image program for Macintosh and plotted as indicated in the graphs on the right panels. Error bars are indicated.

cholesterol-depleted cells a portion of the protein is misfolded.

Role of the ER in Misfolding

Because misfolding occurs only after cholesterol depletion but not after sphingolipid depletion, these data indicate that association of the protein possibly with specialized DRMs in the ER might have a predominant role in its maturation and folding. On the contrary, when the protein has been correctly folded and has reached the Golgi compartment, its conformation is not affected by DRM dissociation obtained either by cholesterol or sphingolipid depletion. To test this hypothesis and to understand whether a relocation of PrP in the ER compartment could per se be responsible for misfolding, we treated FRT cells with brefeldin A (BFA) and checked for protein misfolding.

Indeed, it has been widely shown that Golgi resident proteins (mannosidase II, galactosil-transferase, etc.), Golgi lipid markers (NBD-ceramide), and secretory proteins (e.g., VSV g) all were redistributed into the ER in the presence of BFA (Lippincott-Schwartz *et al.,* 1989; Reaves and Banting 1992; reviewed in Klausner *et al.,* 1992; Wagner *et al.,* 1994; Sciaky *et al.,* 1997). We found that also in FRT cells, under BFA treatment giantin, a Golgi marker, was relocated in the ER compartment and indeed, it lost the characteristic perinuclear cysternal structures (shown in control cells of Figure 7A), while it displayed a punctate-reticular distribution, typical of an ER marker. As expected, BFA treatment also causes a retrograde transport of PrP into the ER, as shown in the double immunofluorescence experiments (Figure 7A) using CLT (ER marker) and giantin (Golgi marker) in Figure 7A. Indeed, although in control cells PrP^C colocalizes with the Golgi marker, it loses its Golgi localization and colocalizes with an ER marker after BFA treatment. Note that although in control conditions a clear plasma membrane signal of PrP is also present, after BFA treatment PrP cannot be visualized on the plasma membrane. This result can be explained because BFA blocks the exocytic transport to the PM but not endocytosis (Prydz *et al.,* 1992).

Interestingly, after BFA treatment PrP^C does not acquire any resistance to PK (Figure 7B) or Triton/Doc insolubility (unpublished data) and does not coimmunoprecipitate with the ER chaperones CNX, CLT, BiP, and PDI (Figure 7C), indicating that ER relocation of the mature protein does not lead to protein misfolding. Thus, it appears that perturbation of the membrane environment by cholesterol depletion during protein synthesis is the direct cause of misfolding.

To test in which specific cellular compartment PrP^C acquires the PK-resistance observed after cholesterol depletion, we separated the ER from the Golgi complex in control and cholesterol-depleted cells using a cell fractionation protocol previously used in FRT cells (Erra *et al.,* 1999; Figure 8).

The postnuclear supernatants of cellular homogenates (from control or Mev/βCD treated cells) were loaded on discontinuous sucrose gradients and after centrifugation (see *Materials and Methods*) collected from the bottom of the tubes in 14 fractions. The sedimentation of the ER and of the *cis*-Golgi derived membranes along these gradients were followed by Western blots using specific antibodies against the ER marker RibI and the Golgi marker GM130 in the different fractions (Figure 8A, top panels). The same fractions were then hybridized with anti-PrP antibody to follow the distribution of the prion protein in these compartments (Figure 8A, bottom panels). As expected, in control conditions PrP^C was prevalently distributed in the fractions enriched in the Golgi marker GM130. On the contrary, after cholesterol depletion PrP^C was enriched in the heavier fractions of the gradient and cosedimented with the ER marker RibI.

Fractions enriched in the ER (fractions 1, 2, and 3) or in the Golgi apparatus (fractions 5, 6, and 7) were pooled and subjected to PK digestion both in control and cholesterol-depleted cells (Figure 8B). Interestingly, we found a PK-resistant band only in the ER-enriched fractions (see Figure 8B), indicating that cholesterol depletion leads to misfolding in this compartment.

DISCUSSION

In this article we have better characterized PrP^C association with DRMs in order to understand its functional role. We have previously shown that perturbation of DRM associa-

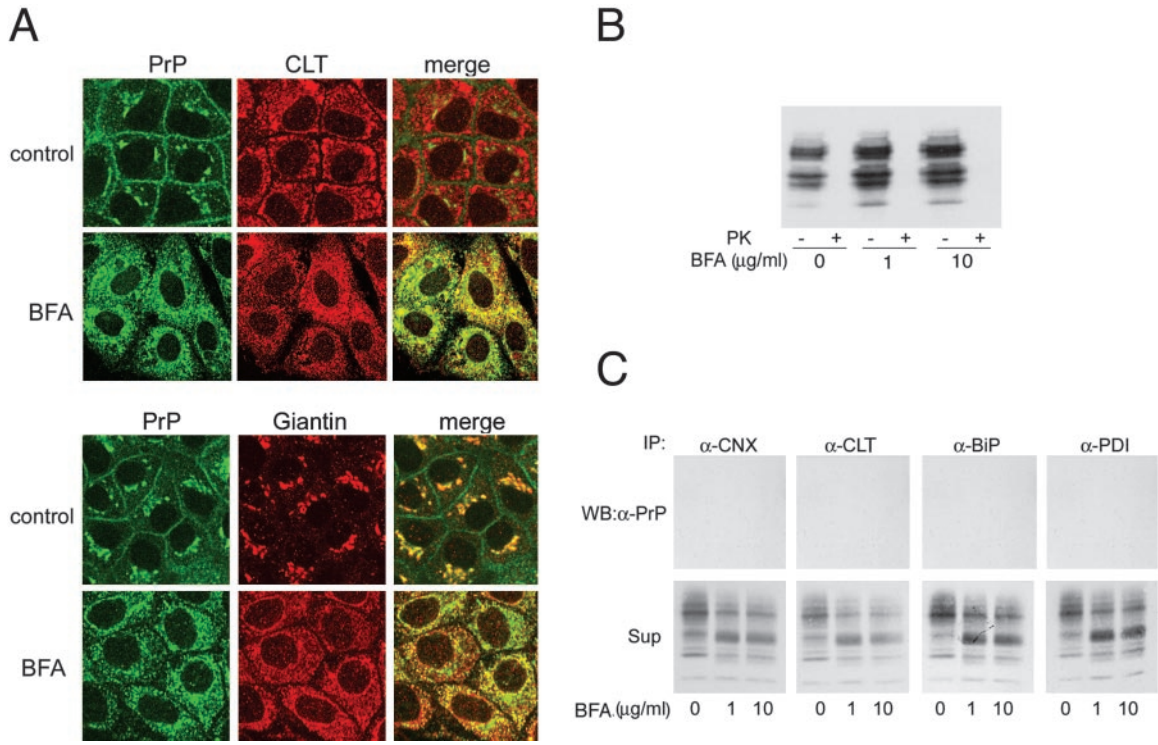

Figure 7. Analysis of PrP^C localization and folding after BFA treatment. (A) Cells were plated on coverslips, in control condition (control) or were treated with BFA (1 μg/ml for 1 h), and then they were subjected to indirect immunofluorescence analysis with anti-PrP, anti-giantin, or anti-CLT antibodies. Secondary antibodies against PrP were TRITC-conjugated, whereas secondary antibodies against giantin and CLT were FITC-conjugated. The images were analyzed by confocal microscopy. (B) Confluent cells on 35-mm dishes were treated for 1 h with different BFA concentrations (0, 1, 10 μg/ml, as indicated) lysed in Triton/Doc and the postnuclear supernatant was treated (+) or not (−) with PK (3.3 μg/ml, 2 min 37°C). PrP^C was revealed by Western blotting with PRI 308 antibody and ECL. (C) Control (0) and BFA (1, 10) treated cells were lysed in JS buffer and CNX, CLT, BiP, and PDI were immunoprecipitated (IP) in nondenaturing conditions with the specific antibodies (see *Materials and Methods*). The immunoprecipitates and 1/10 of the supernatants (Sup) were loaded on polyacrylamide gels. The gels were revealed for the presence of PrP^C in the ER chaperone immunoprecipitated by Western blotting with the antibody against PrP (WB:α-PrP) and ECL analysis.

tion does not affect the sorting and the rate of transport of PrP^C to the plasma membrane in polarized epithelial cells, thus excluding a canonical role for rafts in the exocytic trafficking of this protein (Sarnataro *et al.*, 2002).

By pulse-chase experiments we have demonstrated that PrP^C is always associated with lipid domains from the beginning of its synthesis (Figure 2). Indeed the immature diglycosylated precursor (I*) floats on sucrose gradients already at zero chase time when the protein is completely sensitive to Endo-H treatment, i.e., in a compartment before the medial Golgi.

By subcellular fractionation and ER purification we confirmed that this same isoform is located within DRMs in the ER (Figure 3). This is the first time that association of GPI-anchored proteins to detergent-resistant membrane domains has been reported to occur so early in the secretory pathway of mammalian cells. Indeed, contrary to yeast, where GPI proteins associate with DRMs in the ER (Muniz *et al.*, 2001), in mammalian cells this association is believed to occur only after the protein has become Endo-H resistant (Brown and Rose, 1992; Simons and Ikonen, 1997; S Paladino and C. Zurzolo, unpublished data). It was previously shown that PLAP is in DRM-fractions in the ER of CHO cells (Sevlever *et al.*, 1999).

Interestingly, the different PrP maturation forms show different susceptibility to cholesterol and sphingolipid depletion (see Figure 1). Although DRM association of mature PrP^C (H) is equally perturbed by both cholesterol and sphingolipid depletion, the flotation on sucrose gradients of the immature diglycosylated ER form (I*) is increased by cholesterol depletion, but is decreased by sphingolipid depletion. Consistent with the fact that the major site of sphingolipid synthesis is the Golgi apparatus (Ichikawa and Hirabayashi, 1998; Ohanian and Ohanian, 2001), we believe that the effect of FB1 on flotation of the immature form in the ER might be derived from its effect on the synthesis of ceramide, which has been described as having a major role in promoting raft association and DRM formation (Sutterlin *et al.*, 1997; Cremesti *et al.*, 2002; Sandhoff and Kolter, 2003).

To understand whether DRM association in the ER has a role in PrP^C biosynthesis we performed pulse-chase experiments in conditions of cholesterol and sphingolipid depletion. We found that only in conditions of cholesterol depletion were the kinetics of PrP^C synthesis altered and maturation of the protein slowed down (Figure 4). We also found that in these conditions, but not in control or in sphingolipid-depleted cells, PrP coimmunoprecipitates with ER chaperones (BiP, PDI, CNX, and CLT). These data indicate that in cholesterol-depleted cells PrP^C is folded slowly or could be partially misfolded (see Figure 5).

To directly test for PrP^C misfolding, we performed PK digestion and Triton/Doc insolubility assays, which are also used to assay for scrapie-like properties of the protein (Lehmann and Harris, 1996a, 1996b, 1997; Priola and Chesebro,

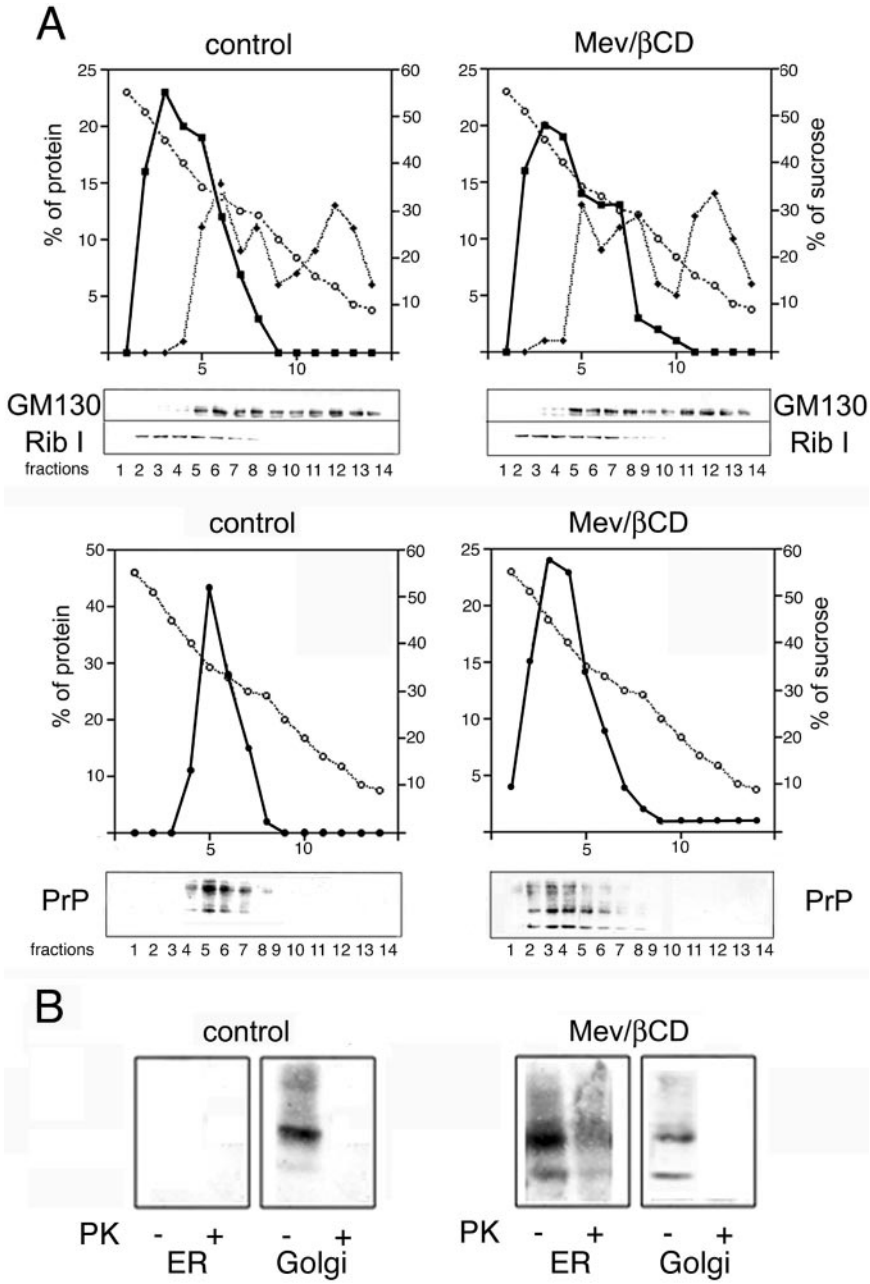

Figure 8. Analysis of the intracellular site of PrP^C misfolding after cholesterol depletion. (A) FRT cells transfected with PrP^C were subjected to cell fractionation in control (control) and cholesterol depletion conditions (Mev/βCD) as described in *Materials and Methods*. The distribution of ER and Golgi markers and PrP^C along the gradient was analyzed. Each fraction was TCA precipitated, run on 12% polyacrylamide gels and analyzed by Western blot and ECL with the antibodies against specific ER and Golgi marker proteins (RibI and GM130) and against PrP. The sucrose concentration in the gradient is indicated with open circles. Gels are shown in the bottom panels, whereas quantitations (RibI, squares; GM130, rhombs; and PrP, filled circles) are shown in top panels. (B) Pooled ER-enriched (1, 2, 3) and Golgi-enriched (5, 6, 7) fractions of the gradients showed in panel A were subjected to PK treatment as previously described. Note that PK-resistant bands are found only in the ER-enriched fractions after cholesterol depletion.

1998). Although in control and FB1-treated cells the protein was totally digested by PK, in conditions of cholesterol depletion PrP^C was partially resistant to PK and was insoluble in Triton/Doc (Figure 6). Interestingly, the band corresponding to the mature protein (H) appeared to be completely digested by PK treatment and was soluble in Triton/Doc, indicating that the portion of the protein that undergoes incorrect folding was derived mainly from the immature form. In addition, by cell fractionation we found that only the PrP fraction cosedimenting with the ER markers acquires an incorrect folding after cholesterol depletion (see Figure 8B). Interestingly it was recently shown that stimulation of PrP^C retrograde transport toward the ER increases the accumulation of PrP^{Sc} in infected cells (Beranger *et al.*, 2002). However, we found that the simple accumulation of the wild-type protein in the ER (by BFA treatment, see Figure 7) does not cause misfolding. Misfolding therefore appears to be a direct consequence of cholesterol depletion. Thus, our data indicate that the different maturation forms are associated to membrane domains differently affected by cholesterol and sphingolipid depletion and that DRM association of the immature PrP precursor in the ER is required for its correct folding. However, when the protein is mature and correctly folded, perturbation of raft-association is not sufficient for misfolding.

The specificity of cholesterol depletion as a cause for misfolding could be explained by two hypotheses: either 1) cholesterol alone could be directly involved in the folding of PrP by acting as a lipochaperone in the ER (Bogdanov and Dowhan, 1999; Sanders and Nagy, 2000; Nomura *et al.*, 2003) or 2) cholesterol depletion leads to a perturbation of the association of the immature form to specific DRMs present

in the ER. The fact that FB1, although altering flotation of the precursor (Figure 1A), does not have any effect on folding led us to postulate that although after FB1 treatment the protein will be surrounded by a different lipid environment, the interaction with cholesterol is nonetheless preserved, and so folding is normal. It will be interesting to investigate whether there is a direct interaction of the different PrP forms with cholesterol. Indeed, specific lipids can play a direct role as chaperones in protein folding (Bogdanov and Dowhan, 1999; Sanders and Nagy, 2000). In particular it has been shown that GM1 binding to β-amyloid (Aβ) results in a conformational transition to a β-sheet structure, supporting the idea that gangliosides may play an important role in modulating the amyloidogenic properties of Aβ (Choo-Smith and Surewicz, 1997).

On the other hand, association with specific membrane domains might directly promote PrP^C folding or indirectly prevent intra- and/or intermolecular PrP interactions of its hydrophobic domains. Indeed, it has been shown that the N-terminal domain of PrP contains a lipid raft targeting determinant (aa23–90; Walmsley *et al.*, 2003) and that another domain, the helix 1 (aa141–171), is the major determinant of PrP folding (Winklhofer *et al.*, 2003). It is possible that during PrP biogenesis its N-terminal region associates directly or indirectly (by protein-protein interactions) with specific DRMs in the ER and that this association is necessary for the subsequent folding of helix 1. One possible explanation for the protein misfolding occurring after cholesterol depletion might therefore be the lack of stabilization of the helix 1 in the absence of DRM association of the N-terminal domain. Indeed, destabilization of helix 1 induces formation of partially PK-resistant aggregates and its deletion leads to block of the glycan maturation of the mutated protein (Winklhofer *et al.*, 2003). Both these features are observed in our experiments after cholesterol depletion (see Figure 4 and 6).

Our finding could be of great importance not only for the normal folding and metabolism of PrP^C, but also for the conversion process. Indeed, Taraboulos *et al.* (1995) have shown that in infected neuroblastoma cells (ScN2a) cholesterol depletion decreases scrapie formation, whereas sphingolipid depletion increases it (Naslavsky *et al.*, 1999). This opposite effect of cholesterol and sphingolipid depletion on scrapie conversion could be explained by the fact that during its life span PrP associates with different types of rafts and therefore the precursor and mature form are differently affected by cholesterol or sphingolipid depletion, as we have shown here.

Our data are only apparently in contrast with the findings that PrP^{Sc} formation is reduced in cholesterol-depleted cells (Taraboulos *et al.*, 1995). Indeed, cholesterol depletion affects both the total level of the mature PrP^C form and the folding of the immature precursor. In both cases, the final result would be a reduction of the substrate for the scrapie conversion reaction. Hence, although the main site of PrP^{Sc} formation might require post-Golgi transport, these and other data present in the literature suggest that the ER can be important in the amplification of PrP^{Sc} formation (Beranger *et al.*, 2002).

Our data could also be relevant in the case of hereditary diseases. Different evidences support the idea that the process of transconformation of PrP with germ-line mutations might begin in the ER (Daude *et al.*, 1997; Harris, 1999) and many PrP mutants are indeed retained in the ER (Lehmann and Harris, 1997; Ivanova *et al.*, 2001). In addition to this, our data suggest that a specific membrane environment (e.g., cholesterol-enriched rafts) of the ER could be important to initiate the transconformational process at this level.

The opposite effect of FB1, which increases PrP^{Sc} production in ScN2a cells (Naslavsky *et al.*, 1999), could also be explained in the light of our findings. Indeed, in our hands FB1 impairs raft-association of the mature form, which could then be more susceptible to undergoing transitional conformation outside rafts in infected cells.

In conclusion our findings allow us to propose a protective role of detergent-resistant domains from misfolding. This is also supported by the recent work of Fantini and colleagues who identified a raft-binding motif ("V3-like domain") that could be involved in the PrP^C to PrP^{Sc} conversion and through which PrP^C can maintain, by interacting with lipid rafts, a nonpathological conformation (Mahfoud *et al.*, 2002). Indeed, binding of PrP to raft-like artificial membranes induces the formation of an α-helical structure (Sanghera and Pinheiro, 2002).

Further experiments are required to clarify the role of rafts in prion replication. In one possible scenario different lipids could act as molecular chaperones to facilitate either the unfolding of one or more α-helices or refolding into β-sheets, a role for which the existence of a molecular chaperone (designated until now as protein X) has already been proposed (Telling *et al.*, 1995). Alternatively, a change in the local environments (in terms of enrichment in specific lipids and proteins) may play the major role in the process. An analytical characterization of the lipid and protein composition of different domains associated with the different PrP^C and PrP^{Sc} forms should shed light on this issue.

ACKNOWLEDGMENTS

We thank Dr. Sylvain Lehmann for the kind gift of the $moPrP^C$ cDNA and helpful discussion. We thank also Drs. Chris Bowler, Andrè Le Bivic, and Stefano Bonatti for critical reading of the manuscript and scientific support. This work was supported by Grants to CZ from MURST, (programmi a cofinanziamento) and from the European Union (HPRN-CT-2000-00077 and QLK-CT-2002-81628) and from Weissman-Pasteur Fondation.

REFERENCES

Bartlett, S.E., Reynolds, A.J., Weible, M., 2nd, Noakes, P.G., and Hendry, I.A. (2001). Transport of endosomal early antigen 1 in the rat sciatic nerve and location in cultured neurons. Neuroreport *12*, 281–284.

Beranger, F., Mange, A., Goud, B., and Lehmann, S. (2002). Stimulation of PrP(C) retrograde transport toward the endoplasmic reticulum increases accumulation of PrP(Sc) in prion-infected cells. J. Biol. Chem. *277*, 38972–38977.

Bogdanov, M., and Dowhan, W. (1999). Lipid-assisted protein folding. J. Biol. Chem. *274*, 36827–36830.

Borchelt, D.R., Scott, M., Taraboulos, A., Stahl, N., and Prusiner, S.B. (1990). Scrapie and cellular prion protein differ in their kinetics of synthesis and topology in cultured cells. J. Cell Biol. *110*, 743–752.

Borchelt, D.R., Taraboulos, A., and Prusiner, S.B. (1992). Evidence for synthesis of scrapie prion proteins in the endocytic pathway. J. Biol. Chem. *267*, 16188–16199.

Brown, D.A., Crise, B., and Rose, J.K. (1989). Mechanism of membrane anchoring affects polarized expression of two proteins in MDCK cells. Science *245*, 1499–1501.

Brown, D.A., and London, E. (1998). Functions of lipid rafts in biological membranes. Annu. Rev. Cell Dev. Biol. *14*, 111–136.

Brown, D.A., and Rose, J.H. (1992). Sorting of GPI-anchored proteins to glycolipid-enriched membrane subdomains during transport to the apical cell surface. Cell *68*, 533–544.

Capellari, S., Zaidi, S.I.A., Urig, C.B., Perry, G., Smith, M.A., and Petersen, R.B. (1999). Prion protein glycosylation is sensitive to redox change. J. Biol. Chem. *274*, 34846–34850.

Caughey, B., Race, R.E., Ernst, D., Buchmeier, M.J., and Chesebro, B. (1989). Prion protein biosynthesis in scrapie-infected and uninfected neuroblastoma cells. J. Virol. *63*, 175–181.

Caughey, B., and Raymond, G.J. (1991). The scrapie-associated form of PrP is made from a cell surface precursor that is both protease- and phospholipase-sensitive. J. Biol. Chem. *266*, 18217–18223.

Caughey, B., Raymond, G.J., Ernst, D., and Race, R.E. (1991). N-terminal truncation of the scrapie-associated form of PrP by lysosomal protease(s): implication regarding the site of conversion of PrP to the protease-resistant state. J. Virol. *65*, 6597–6603.

Chabry, J., Priola, S.A., Wehrly, K., Nishio, J., Hope, J., and Chesebro, B. (1999). Species-independent inhibition of abnormal prion protein (PrP) formation by a peptide containing a conserved PrP sequence. J. Virol. *73*, 6245–6250.

Choo-Smith, L.P., and Surewicz, W.K. (1997). The interaction of the Alzheimer amyloid beta peptide and ganglioside GM1-containing membranes. FEBS Lett. *402*, 95–98.

Cremesti, A.E., Goni, F.M., and Kolesnick, R. (2002). Role of sphingomyelinase and ceramide in modulating rafts: do biophysical properties determine biologic outcome? FEBS Lett. *531*, 47–53.

Daude, N., Lehmann, S., and Harris, D.A. (1997). Identification of intermediate steps in the conversion of a mutant prion protein to a scrapie-like form in cultured cells. J. Biol. Chem. *272*, 11604–11612.

Dhanvantari, S., and Loh, Y.P. (2000). Lipid raft association of carboxypeptidase E is necessary for its function as a regulated secretory pathway sorting receptor. J. Biol. Chem. *275*, 29887–29893.

Erra, M.C., Iodice, L., Lotti, L.V., and Bonatti, S. (1999). Cell fractionation analysis of human CD8 glycoprotein transport between endoplasmic reticulum, intermediate compartment and Golgi complex in tissue cultured cells. Cell. Biol. Intern. *23*, 571–577.

Harris, D.A. (1999). Cellular biology of prion diseases. Clin. Microbiol. Rev. *12*, 429–444.

Horiuchi, M., and Caughey, B. (1999). Specific binding of normal prion protein to the scrapie form via a localized domain initiates its conversion to the protease-resistant state. EMBO J. *18*, 3193–3203.

Ichikawa, S., and Hirabayashi, Y. (1998). Glucosylceramide synthase and glycosphingolipid synthesis. Trends Cell Biol. *8*, 198–202.

Ivanova, L., Barmada, S., Kummer, T., and Harris, D.A. (2001). Mutant prion proteins are partially retained in the endoplasmic reticulum. J. Biol. Chem. *276*, 42409–42421.

Jackson, M.R., Cohen-Doyle, M.F., Peterson, P.A., and Williams, D.B. (1994). Regulation of MHC class I transport by the molecular chaperone, calnexin (p88, IP90). Science *263*, 384–387.

Jeffrey, M., McGovern, G., Goodsir, C.M., Brown, K.L., and Bruce, M.E. (2000). Sites of prion protein accumulation in scrapie-infected mouse spleen revealed by immuno-electron microscopy. J. Pathol. *191*, 323–332.

Kaneko, K., Vey, M., Scott, M., Pilkuhn, S., Cohen, F.E., and Prusiner, S.B. (1997). COOH-terminal sequence of the cellular prion protein directs subcellular trafficking and controls conversion into the scrapie isoform. Proc. Natl. Acad. Sci. USA *94*, 2333–2338.

Kauppi, M., Simonsen, A., Bremnes, B., Vieira, A., Callaghan, J., Stenmark, H., and Olkkonen, V.M. (2002). The small GTPase Rab22 interacts with EEA1 and controls endosomal membrane trafficking. J. Cell Sci. *115*(Pt 5), 899–911.

Keller, P., and Simons, K. (1998). Cholesterol is required for surface transport of influenza virus hemagglutinin. J. Cell Biol. *140*, 1357–1367.

Klausner, R.D., Donaldson, J.G., and Lippincott-Schwartz, J. (1992). Brefeldin A: insights into the control of membrane traffic and organelle structure. J. Cell Biol. *116*, 1071–1080.

Klein, T.R., Kirsch, D., Kaufmann, R., and Riesner, D. (1998). Prion rods contain small amounts of two host sphingolipids as revealed by thin-layer chromatography and mass spectrometry. Biol. Chem. *379*, 655–666.

Kocisko, D.A., Come, J.H., Priola, S.A., Chesebro, B., Raymond, G.J., Lansbury, P.T., and Caughey, B. (1994). Cell-free formation of protease-resistant prion protein. Nature *370*, 471–474.

Kuzchalia, T.V., and Parton, R.G. (1999). Membrane microdomains and caveolae. Curr. Opin. Cell Biol. *11*, 424–431.

Laszlo, L. *et al.* (1992). Lysosomes as key organelles in the pathogenesis of prion encephalopathies. J. Pathol. *166*, 333–341.

Lehmann, S., and Harris, D.A. (1996a). Two mutant prion proteins expressed in cultured cells acquire biochemical properties reminiscent of the scrapie isoform. Proc. Natl. Acad. Sci. USA *93*, 5610–5614.

Lehmann, S., and Harris, D.A. (1996b). Mutant and infectious prion proteins display common biochemical properties in cultured cells. J. Biol. Chem. *271*, 1633–1637.

Lehmann, S., and Harris, D.A. (1997). Blockade of glycosylation promotes acquisition of scrapie-like properties by the prion protein in cultured cells. J. Biol. Chem. *272*, 21479–21487.

Lipardi, C., Nitsch, L., and Zurzolo, C. (2000). Detergent insoluble GPI-anchored proteins are apically sorted in Fisher rat thyroid cells, but interference with cholesterol or sphingolipids differentially affects detergent insolubility and apical sorting. Mol. Biol. Cell *11*, 531–542.

Lippincott-Schwartz, J., Yuan, L.C., Bonifacino, J.S., and Klausner, R.D. (1989). Rapid redistribution of Golgi proteins into the ER in cells treated with brefeldin A: evidence for membrane cycling from Golgi to ER. Cell *56*, 801–813.

Lisanti, M.P., Caras, J.W., Davitz, M.A., and Rodriguez-Boulan, E. (1989). A glycophospholipid membrane anchor acts as an apical targeting signal in polarized epithelial cells. J. Cell Biol. *109*, 2145–2156.

Ma, J., and Lindquist, S. (2001). Wild-type and mutant associated with prion disease are subjected to retrograde transport and proteasome degradation. Proc. Natl. Acad. Sci. USA *98*, 4955–4960.

Ma, J., and Lindquist, S. (2002). Conversion of PrP to a self-perpetuating PrP^{Sc}-like conformation in the cytosol. Science *298*, 1785–1788.

Ma, J., Wollmann, R., and Lindquist, S. (2002). Neurotoxicity and neurodegeneration when PrP accumulates in the cytosol. Science *298*, 1781–1785.

Magalhaes, A.C., Silva, J.A., Lee, K.S., Martins, V.R., Prado, V.F., Ferguson, S.S., Gomez, M.V., Brentani, R.R., and Prado, M.A. (2002). Endocytic intermediates involved with the intracellular trafficking of a fluorescent cellular prion protein. J. Biol. Chem. *277*, 33311–33318.

Mahfoud, R., Garmy, N., Maresca, M., Yahi, N., Puigserver, A., and Fantini, J. (2002). Identification of a common sphingolipid-binding domain in Alzheimer, Prion and HIV proteins. J. Biol. Chem. *277*, 11292–11296.

Mayor, S., and Maxfield, F.R. (1995). Insolubility and redistribution of GPI-anchored proteins at the cell surface after detergent treatment. Mol. Biol. Cell *6*, 929–944.

Muniz, M., Morsomme, P., and Riezman, H. (2001). Protein sorting upon exit from endoplasmic reticulum. Cell *104*, 313–320.

Nakamura, N., Rabouille, C., Watson, R., Nilsson, T., Hui, N., Slusarewicz, P., Kreis, T.E., and Warren, G. (1995). Characterization of a cis-Golgi matrix protein, GM130. J. Cell Biol. *131*(6, Pt 2), 1715–1726.

Narindrasorasak, S., Yao, P., and Sarkar, B. (2003). Protein disulfide isomerase, a multifunctional protein chaperone, shows copper-binding activity. Biochem. Biophys. Res. Commun. *311*, 405–414.

Naslavsky, N., Shmeeda, H., Friedlander, G., Yanai, A., Futerman, A.H., Barenholz, Y., and Taraboulos, A. (1999). Sphingolipid depletion increases formation of the scrapie prion protein in neuroblastoma cells infected with prions. J. Biol. Chem. *274*, 20763–20771.

Naslavsky, N., Stein, R., Yanai, A., Friedlander, G., and Taraboulos, A. (1997). Characterization of detergent-insoluble complex containing the cellular prion protein and its scrapie isoform. J. Biol. Chem. *272*, 6324–6331.

Nigam, S.K. (1990). Subcellular distribution of small GTP binding proteins in pancreas: identification of small GTP binding proteins in the rough endoplasmic reticulum. Proc. Natl. Acad. Sci. USA *87*, 1296–1299.

Nomura, Y., Ikeda, M., Yamaguchi, N., Aoyama, Y., and Akiyoshi, K. (2003). Protein refolding assisted by self-assembled nanogels as novel artificial molecular chaperone. FEBS Lett. *553*, 271–276.

Ohanian, J., and Ohanian, V. (2001). Sphingolipids in mammalian cell signalling. Cell Mol. Life Sci. *58*, 2053–2068.

Parton, R.G. (1994). Ultrastructural localization of gangliosides; GM1 is concentrated in caveolae. J. Histochem. Cytochem. *42*, 155–166.

Paulsson, K., and Wang, P. (2003). Chaperones and folding of MHC class I molecules in the endoplasmic reticulum. Biochim. Biophys. Acta *1641*, 1–12.

Petersen, R.B., Parchi, P., Richardson, S.L., Urig, C.B., and Gambetti, P. (1996). Effect of the D178N mutation and the codon 129 polymorphism on the metabolism of the prion protein. J. Biol. Chem. *271*, 12661–12668.

Piccardo, P. *et al.* (1998). An antibody raised against a conserved sequence of the prion protein recognizes pathological isoforms in human and animal prion diseases, including Creutzfeldt-Jakob disease and bovine spongiform encephalopathy. Am. J. Pathol. *152*, 1415–1420.

Prado, M.A.M., Alves-Silva, J., Magalhaes, A.C., Prado, V.F., Linden, R., Martins, V.M., and Brentani, R.R. (2004). PrP^{C} on the road: trafficking of the cellular prion protein. J. Neurochem. *88*, 769–781.

Priola, S.A., and Chesebro, B. (1998). Abnormal properties of prion protein with insertional mutations in different cell types. J. Biol. Chem. *273*, 11980–11985.

Prydz, K., Hansen, S.H., Sandvig, K., and van Deurs, B. (1992). Effects of brefeldin A on endocytosis, transcytosis and transport to the Golgi complex in polarized MDCK cells. J. Cell Biol. *119*, 259–272.

Prusiner, S.B., Scott, M.R., deArmond, S.J., and Cohen, F.E. (1998). Prion protein biology. Cell *93*, 337–348.

Reaves, B., and Banting, G. (1992). Perturbation of the morphology of the trans-Golgi network following Brefeldin A treatment: redistribution of a TGN-specific integral membrane protein, TGN38. J. Cell Biol. *116*, 85–94.

Sanders, C.R., and Nagy, J.K. (2000). Misfolding of membrane proteins in health and disease: the lady or the tiger? Curr. Opin. Struct. Biol. *10*, 438–442.

Sandhoff, K., and Kolter, T. (2003). Biosynthesis and degradation of mammalian glycosphingolipids. Philos. Trans. R. Soc. Lond. B. Biol. Sci. *358*, 847–861.

Sanghera, N., and Pinheiro, T.J. (2002). Binding of prion protein to lipid membranes and implication for prion replication. J. Mol. Biol. *315*, 1241–1256.

Sarnataro, D., Paladino, S., Campana, V., Grassi, J., Nitsch, L., and Zurzolo, C. (2002). PrP^{C} is sorted to the basolateral membrane of epithelial cells independently of its association with rafts. Traffic *3*, 810–821.

Sciaky, N., Presley, J., Smith, C., Zaal, K.J., Cole, N., Moreira, J.E., Terasaki, M., Siggia, E., and Lippincott-Schwartz, J. (1997). Golgi tubule traffic and the effects of brefeldin A visualized in living cells. J. Cell Biol. *139*, 1137–1155.

Sevlever, D., Pickett, S., Mann, K.J., Sambamurti, K., Medof, M.E., and Rosenberry, T.L. (1999). Glycosylphosphatidylinositol-anchor intermediates associate with triton-insoluble membranes in subcellular compartments that include the endoplasmic reticulum. Biochem. J. *343*, 627–635.

Shyng, S-L., Heuser, J.E., and Harris, D.A. (1994). A glycolipid-anchored prion protein is endocytosed via clathrin-coated pits. J. Cell Biol. *125*, 1239–1250.

Simons, K., and Ikonen, E. (1997). Functional rafts in cell membrane. Nature *387*, 569–572.

Sutterlin, C., Doering, T.L., Schimmoller, F., Schroder, S., and Riezman, H. (1997). Specific requirements for the ER to Golgi transport of GPI-anchored proteins in yeast. J. Cell Sci. *110*(Pt 21), 2703–2714.

Taguchi, T., Pypaert, M., and Warren, G. (2003). Biochemical sub-fractionation of the Mammalian Golgi apparatus. Traffic *4*, 344–352.

Taraboulos, A., Raeber, A.J., Borchelt, D.R., Serban, D., and Prusiner, S.B. (1992). Synthesis and trafficking of prion proteins in cultured cells. Mol. Biol. Cell *3*, 851–863.

Taraboulos, A., Scott, M.R.D., Semenov, A., Avraham, D., Laszlo, L., and Prusiner, S.B. (1995). Cholesterol depletion and modification of COOH terminal targeting sequence of the prion protein inhibit formation of the scrapie isoform. J. Cell Biol. *129*, 121–132.

Telling, G.C., Scott, M., Mastrianni, J., Gabizon, R., Torchia, M., Cohen, F.E., DeArmond, S.J., and Prusiner, S.B. (1995). Prion propagation in mice expressing human and chimeric PrP transgenes implicates the interaction of cellular PrP with another protein. Cell *83*, 79–90.

Thotakura, N.R., and Bahl, O.P. (1987). Enzymatic deglycosylation of glycoproteins. Methods Enzymol. *138*, 350–359.

Tiveron, M.C., Nosten-Bertrand, M., Jani, H., Garnett, D., Hirst, E.M., Grosveld, F., and Morris, R.J. (1994). The mode of anchorage to the cell surface determines both the function and the membrane location of Thy-1 glycoprotein. J. Cell Sci. *107*, 1783–1796.

van der Goot, F.G., and Harder, T. (2001). Rafts membrane domains: from a liquid-ordered membrane phase to a site of pathogen attack. Semin. Immunol. *13*, 89–97.

Vey, M., Pilkuhn, S., Wille, H., Nixon, R., DeArmond, S.J., Smart, E.J., Anderson, R.G., Taraboulos, A., and Prusiner, S.B. (1996). Subcellular colocalization of the cellular and scrapie prion proteins in caveolae-like membranous domains. Proc. Natl. Acad. Sci. USA *93*, 14945–14949.

Wagner, M., Rajasekanaran, A.K., Hanzel, D.K., Mayor, S., and Rodriguez-Boulan, E. (1994). Brefeldin A causes structural and functional alterations of the trans-Golgi network of MDCK cells. J. Cell Sci. *107*, 933–943.

Walmsley, A.R., Zeng, F., and Hooper, N.M. (2003). The N-terminal region of the prion protein ectodomain contains a lipid raft targeting determinant. J. Biol. Chem. *278*, 37241–37248.

Winklhofer, F., Heske, J., Heller, U., Reintjes, A., Muranyi, W., Moarefi, I., and Tatzelt, J. (2003). Determinants of the in vivo folding of the prion protein. A bipartite function of helix 1 in folding and aggregation. J. Biol. Chem. *278*, 14961–14970.

Wopfner, F., Weidenhofer, G., Schneider, R., von Brunn, A., Gilch, S., Schwarz, T.F., Werner, T., and Schatzl, H.M. (1999). Analysis of 27 mammalian and 9 avian PrPs reveals high conservation of flexible regions of the prion protein. J. Mol. Biol. *289*, 1163–1178.

Ying, M., Flatmark, T., and Saraste, J. (2000). The p58-positive pre-golgi intermediates consist of distinct subpopulations of particles that show differential binding of COPI and COPII coats and contain vacuolar H(+)-ATPase. J. Cell Sci. *11*(Pt 20), 3623–3638.

Zurzolo, C., Lisanti, M.P., Caras, I.W., Nitsch, L., and Rodriguez-Boulan, E. (1993). Glycosylphosphatidylinositol-anchored proteins are preferentially targeted to the basolateral surface in Fischer rat thyroid epithelial cells. J. Cell Biol. *121*, 1031–1039.

Zurzolo, C., van't Hof, W., Van Meer, G., and Rodriguez-Boulan, E. (1994). VIP21/caveolin, glycosphingolipid clusters and the sorting of glycosylphosphatidylinositol-anchored proteins in epithelial cells. EMBO J. *13*, 42–53.